Specific Emitter Identification Based on Intrinsic Time-Scale-Decomposition and Image Texture Feature

Dongfang Ren, Tao Zhang
Zhengzhou Information Science and Technology Institute
Zhengzhou, China
e-mail: rendongf197@163.com, zhangtao_brunda@163.com

***Abstract*—Specific emitter identification (SEI) aims at discerning radio emitters using external measurement features called the radio frequency (RF) fingerprints of the signal. SEI is widely used in intelligent gathering, network intrusion detection, Cognitive Radio and so on. In this paper, we proposed a novel SEI method based on steady signals, which is more practical. We firstly get the time-frequency-energy distribution (TFED) of the signal using Intrinsic Time-scale Decomposition(ITD), which is more suitable for non-stationary signal than empirical mode decomposition (EMD).Secondly, we transform the TFED of the signal into a gray image and several image texture features are extracted from histogram statistics and Gray-Level Co-Occurrence Matrix (GLCM) of the image. We treat these texture features as the signal's RF fingerprints to identify the specific emitter. Measured ship signals and simulated signals are used to evaluate the performance of the proposed method and another two methods are compared with it. Experimental results demonstrate that the proposed method is more effective.**

Keywords-SEI; TFED spectrum; ITD; texture features

I. INTRODUCTION

Specific emitter identification (SEI) [1] , which identifies the individual communication equipment by the radio frequency (RF) fingerprints of signals [2], is a hot research topic in battlefield management, intelligence gathering [3], cognitive radio network intrusion detection [4], etc. The SEI technique has been studied and used in military filed recent years, which has become increasingly important in providing reliable and timely electronic intelligence about the important communication equipments of enemy.

Based on previous researches, SEI utilizes transient or stable signal to measure the features and discern communication equipment. Transient signal occur when an emitter is turned on or switched modes, reflecting the nonlinear combination of components such as diodes, triodes, amplifiers in a emitter. So, transient signal can provide distinguishable characteristics among different emitters. In previous researches, the transient signal features were mainly extracted from the instantaneous amplitude, phase, frequency and energy envelope. However, due to the short duration and susceptibility, accurate detection and acquisition of transient signal are vital to identification results, which restrict the utilization of transient signal in practice.

Stable signal is produced by emitters under stable condition. Although the individual characteristics of emitter are driven in the modulating signal, resulting many difficulties in extraction, the stable signal is easily detected and captured on account of the long duration [5]. Therefore, SEI technique based on stable signal has more practical application. Several methods extracting nonlinear features from the stable signal have been researched such as bispectrum, fractal dimension, time-frequency analysis, etc. which get good identification performance.

Among all the methods mentioned above, time-frequency analysis reveals 2-D information about signal in time domain and frequency domain simultaneously, which provides more subtle features about similar emitter signals. The common time-frequency analysis methods include short-time Fourier transform, Wavelet Transform, Wigner-Ville and Choi-Williams distribution [6]. Several drawbacks exist in these methods, affecting their application in SEI. A new time-frequency analysis method named Hilbert-Huang transform proposed by Huang et al. [7] can decompose the signal self-adoptively. It's suitable to analyze the non-stationary signal because it provides a relatively precise TFED without any prior information about the signal. But these papers [8] [9] point out that there are several drawbacks in empirical mode decomposition (EMD). The process of obtaining intrinsic mode functions (IMFs) in EMD is inefficient and there are serious boundary effects in it. What' more, the process of EMD produces some new components that does not exist in the raw signal.

Mark G. Frei and Ivan Osorio proposed the ITD for TFED analysis in 2007 [9]. The ITD overcomes the limitation of EMD, improves both accuracy and efficiency in the acquisition of TFED, which is specifically formulated for nonlinear or non-stationary signals. Precise temporal information acquisition makes it more useful in SEI [10]. We acquire the TFED of emitter signals by ITD firstly. Then, we transform the TFED spectrum into a grey image. Finally, we extract several texture features from the grey image as RF fingerprints for SEI. To test the performance of proposed algorithm, another two methods based on EMD are used to compare with it. The experimental results demonstrate that the proposed algorithm achieves better recognition accuracy.

The rest of the paper is organized as follows. In Section II, the ITD method is firstly introduced, and then we explain the acquisition of TFED. In Section III, we introduce the extraction of RF fingerprints and support vector machine (SVM). Experimental results are depicted in Section IV. In

978-1-5090-3822-0/17/$31.00 ©2017 IEEE

Authorized licensed use limited to: ULAKBIM UASL - Bogazici Universitesi. Downloaded on December 07,2020 at 21:24:35 UTC from IEEE Xplore. Restrictions apply.

section V, we draw the conclusion and make a summary and outlook finally.

II. EXTRACTION OF TFED SPECTRUM

A. Intrinsic Time-Scale Decomposition

Given a real-value signal X_t, we define an operator L, which extracts a baseline signal from X_t and leaves the residual to be a proper rotation. We can express the X_t as

$$X_t = LX_t + (1-L)X_t = L_t + H_t, \tag{1}$$

where $L_t = LX_t$ is the baseline signal and $H_t = (1-L)X_t$ is a proper rotation.

Here, we define $\{\tau_k, k=1,2,3...\}$ as the local extrema of real-value signal and define $\tau_0 = 0$ for convenience. If some intervals of X_t are constant but contain extrema due to fluctuations in adjacent signal, τ_k is chosen as the right endpoint of the interval. To simplify the notation, let X_k and L_k denote $X(\tau_k)$ and $L(\tau_k)$, respectively.

Suppose that L_t and H_t have been defined on $[0, \tau_k]$ and X_t is available for $[0, \tau_{k+2}]$. We define a baseline-extracting operator L, on the interval $(\tau_k, \tau_{k+1}]$ between successive extrema as follows:

$$LX_t = L_t = L_k + (\frac{L_{k+1} - L_k}{X_{k+1} - X_k})(X_t - X_k), \tag{2}$$

$$L_{k+1} = \alpha[X_k + (\frac{\tau_{k+1} - \tau_k}{\tau_{k+2} - \tau_{k+1}})(X_t - X_k)] + (1-\alpha)X_{k+1}, \tag{3}$$

and $0<\alpha<1$ is usually set at 0.5. To initialize the decomposition on the interval $[0, \tau_1]$ (suppose $\tau_0 = 0$), the first value of baseline signal L_t is defined as $L_0 = (X_{\tau_0} + X_{\tau_1})/2$. After defining the baseline signal according to equations (2) and (3), we can also define the proper-rotation extracting operator H, as

$$HX_t = (1-L)X_t = H_t = X_t - L_t. \tag{4}$$

The proper rotation components produced by the ITD is not unique due to the choice of α. Once the input signals is decomposed into a baseline component and a proper rotation component, the decomposition process can be re-applied regarding the baseline signal as the input. This procedure can be iterated until the stopping criterion is satisfied that max decomposition time or a monotonic baseline signal is obtained. The original signal is decomposed into a sequence of proper rotations at each subsequent level of decomposition. More precisely,

$$\begin{aligned} X_t &= HX_t + LX_t = HX_t + (H+L)LX_t = (H(1+L) + L^2)X_t \\ &= (H\sum_{k=0}^{p-1} L^k + L^p)X_t, \end{aligned} \tag{5}$$

where $HL^k X_t$ is the $(k+1)th$ level proper rotation and $L^p X_t$ is the baseline component .Baseline component is either the monotonic trend or the lowest frequency component if the decomposition is stopped before the monotonic trend is reached. Then, we can extract the instantaneous information from component signals. The traditional instantaneous amplitude, phase and frequency are obtained by Hilbert transform as follows:

$$\left.\begin{aligned} A_t &= |R_t + ih[R_t]| \\ \theta_\tau &= angle(R_t + ih[R_t]) \\ f_t &= \frac{1}{2\pi}\frac{d\theta_\tau}{dt} \end{aligned}\right\}, \tag{6}$$

where $h[R_t]$ represents the Hilbert transform. However, there are some difficulties in Hilbert transform-based approach to TFED analysis for its edge effects, non-recursive nature and the occasion appearance of negative frequencies, which should not for proper rotations. Two useful alternatives for determining instantaneous amplitude, phase and frequency are introduced as follows:

$$\theta_t^1 = \begin{cases} \sin^{-1}(\frac{x_t}{A_1}), t \in [t_1, t_2) \\ \pi - \sin^{-1}(\frac{x_t}{A_1}), t \in [t_2, t_3) \\ \pi - \sin^{-1}(\frac{x_t}{A_2}), t \in [t_3, t_4) \\ 2\pi + \sin^{-1}(\frac{x_t}{A_2}), t \in [t_4, t_5) \end{cases}, \tag{7}$$

and

$$\theta_t^2 = \begin{cases} \frac{x_t}{A_1}\frac{\pi}{2}, t \in [t_1, t_2) \\ \frac{x_t}{A_1}\frac{\pi}{2} + (1 - \frac{x_t}{A_1})\pi, t \in [t_2, t_3) \\ (-\frac{x_t}{A_2})\frac{3\pi}{2} + (1 + \frac{x_t}{A_2})\pi, t \in [t_3, t_4) \\ (-\frac{x_t}{A_2})\frac{3\pi}{2} + (1 + \frac{x_t}{A_2})2\pi, t \in [t_4, t_5) \end{cases}, \tag{8}$$

where $A_1 > 0$ and $A_2 > 0$ are the adjacent amplitudes of the positive and negative half-waves. The relationship and the position among parameters above are illustrated in Figure 1.

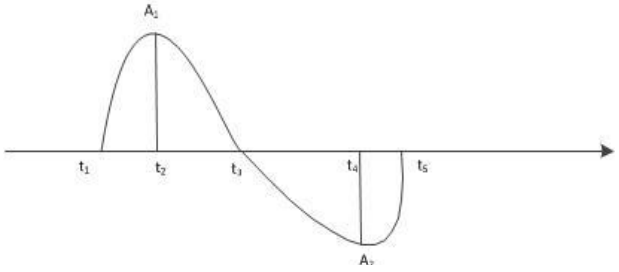

Figure 1. Illustration of the parameters and position.

The instantaneous amplitude is determined by the

Authorized licensed use limited to: ULAKBIM UASL - Bogazici Universitesi. Downloaded on December 07,2020 at 21:24:35 UTC from IEEE Xplore. Restrictions apply.

extrema values of the proper rotations between zero crossings as follows：

$$A_t^1 = A_t^2 = \begin{cases} A_1, t \in [t_1, t3) \\ -A_2, t \in [t_3, t5) \end{cases}. \quad (9)$$

We can obtain the instantaneous frequency from the phase by (6). Compared with the Hilbert transform, these two methods can accurately express the dynamic characters of the non-stationary signals.

B. TFED Spectrum Analysis

As mentioned above, the decomposition process does not stop until a monotonic baseline signal is obtained or the max decomposition level is reached. Considering the computation complexity and analytical precision, we set the max decomposition level at 5 and calculate the instantaneous amplitude and frequency of each component. Based on the instantaneous information, we can get the TFED spectrum in a way similar to HHT [7]. We use the matrix $I_{ij}(w,t)$, i=1… N_t, j=1… N_f, to represent the whole TFED spectrum obtained by ITD method, where N_t represents the number of rows, N_f represents the number of columns. Several RF fingerprints can be extracted from the TFED spectrum for SEI.

III. RF FINGERPRINT EXTRACTION AND CLASSIFICATION

A. Image Texture Features Extraction

Image texture feature is a kind of visual feature based on content, which is widely applied in image description and categorization [11]. Firstly, we convert the TFED spectrum into a gray image as:

$$\mathbf{X}_{i,j} = \text{round}[\frac{\mathbf{I}_{i,j}}{\max \mathbf{I}_{i,j}} \times 255]. \quad (10)$$

where $\mathbf{I}_{i,j}$ is the $(i,j)th$ value of the TFED spectrum matrix. $\mathbf{X}_{i,j}$ is the $(i,j)th$ value of the image matrix $\mathbf{X}$ and $round[*]$ is the function rounds the value to the nearest integers. The whole TFED spectrum is linearly scaled to integers ranging from 0 to 255. We can extract several image texture features of TFED spectrums by calculating histogram statics and GLCM.

1) Histogram statistics features

For a gray image matrix $X_{i,j}$ derived from TFED spectrums, we compute the normalized histogram statistics as

$$P(l) = \frac{N(l)}{M}, l = 0,1...255. \quad (11)$$

where l is the gray-level value, $N(l)$ is the number of l in matrix $\mathbf{X}_{i,j}$, and M is the total number of elements in matrix $\mathbf{X}_{i,j}$ .So we can extract six features from the $P(l)$ as follows:

The mean of gray image

$$V_1 = \sum_{l=1}^{255} l * p(l), \quad (12)$$

The variance of gray image

$$V_2 = \sum_{l=0}^{255} (l - V_1)^2 * p(l), \quad (13)$$

The skewness of gray image

$$V_3 = \frac{1}{V_2^{\frac{3}{2}}} * \sum_{l=0}^{255} (V_1 - l)^3 * p(l), \quad (14)$$

The kurtosis of gray image:

$$V_4 = \frac{1}{V_2^2} * \sum_{l=0}^{255} (V_1 - l)^4 * p(l), \quad (15)$$

The energy of histogram:

$$V_5 = \sum_{l=0}^{255} p(l)^2, \quad (16)$$

The entropy of histogram

$$V_6 = -\sum_{l=0}^{255} p(l) * lnp(l), \quad (17)$$

2) GLCM features

The GLCM describes the texture features based on the position relationship between pixels, which is widely used in the texture features extraction of medical and remote sensing image. The GLCM can be calculated as follows:

$$p(l_1, l_2) = \frac{\sum \{[(x_1, y_1), (x_2, y_2)] \in Q \mid f(x_1, y_1) = l_1 \& f(x_2, y_2) = l_2\}}{\sum [(x_1, y_1), (x_2, y_2) \in Q]}, \quad (18)$$

$p(l_1, l_2)$ is a 2-D function and l_1, l_2 represent pixel pair with gray-level value l_1 and l_2 .The denominator in the formula above represents the total number of pixels pair and the numerator represents the number of pixel pair with gray-level value l_1 and l_2 .Besides, Q represents a kind of location relationship between a pair of pixels. We usually use a two-element vector containing row offset and column offset to describe this relationship of pixels pair. Here we use [0, 1], [-1, 1], [-1, 0] and [-1, -1] to get 4 different GLCMs. To ensure accuracy while reducing computational complexity, we set the gray-level of the GLCM at 64 instead of 256 and normalize it. So, the size of GLCM is 64×64 and 4 features are extracted from each GLCM. For the GLCM whose offset is [0, 1], 4 features are extracted as follows:

The contrast of the whole image:

$$V_7 = -\sum_{l_1=1}^{64} \sum_{l_2=1}^{64} p(l_1, l_2) * (l_1 - l_2)^2, \quad (19)$$

The correlation of a pixel with its neighbor over the whole image:

$$V_8 = \sum_{l_1=1}^{64} \sum_{l_2=1}^{64} \frac{(l_1 - \mu_1^{l_1}) * (l_2 - \mu_2^{l_2}) * p(l_1, l_2)}{\sigma_1^{l_1} \sigma_2^{l_2}}, \quad (20)$$

Authorized licensed use limited to: ULAKBIM UASL - Bogazici Universitesi. Downloaded on December 07,2020 at 21:24:35 UTC from IEEE Xplore. Restrictions apply.

$\mu_1^{l_1}$ and $\mu_2^{l_2}$ are the mean of the $l_1 th$ row and the $l_2 th$ column in GLCM, respectively. $\sigma_1^{l_1}$ and $\sigma_2^{l_2}$ are the standard deviation of $l_1 th$ row and $l_2 th$ column.

The energy of GLCM:

$$V_9 = \sum_{l_1=1}^{64}\sum_{l_2=1}^{64} p(l_1,l_2)^2, \tag{21}$$

The homogeneity of GLCM:

$$V_{10} = \sum_{l_1=1}^{64}\sum_{l_2=1}^{64} \frac{p(l_1,l_2)}{1+|l_1-l_2|}, \tag{22}$$

here we extract 16 features totally from 4 GLCMs. Combined with six features extracted from histogram statistics, 22 texture features are acquired to describe the RF fingerprints of stable signals for SEI.

B. Classification

Based on the 22 texture features of TFED spectrum, we use support vector machine (SVM) to identify different emitter signals [12]. SVM is a common supervised classification method, widely used in analysis of regression and data prediction, which plays an important role in solving the pattern recognition problems with high dimension, nonlinearity and few samples. In this paper, we use a SVM toolbox LIBSVM 3.20 to fulfill our experiments. Besides, the Cross Validation (CV) is used to find best parameters in SVM. CV is a statistical analysis method for validating the performance of classifiers, which divides the original dataset into the training set and the validation set. We train a classifier first using the training dataset and then test the performance of classifier by the validation set. The recognition accuracy is the performance indicator for finding best parameters.

IV. Experimental Design and Results

A. Comparative Methods and Signal Acquisition

In this section, we test the identification performance of the proposed method with another two methods. Zhang et al. [13] introduce 3 methods based on HHT for SEI, one of which relies on the energy entropy, first-order moment and second-order moment of the Hilbert spectrum as features for SEI. We call it the comparative Method 1. Yuan et al. [14] introduce a method for SEI, which extracts 13 TFED features from transient signal. We remove 3 features, sum of energy, duration of transient signal and duration of maximum energy point, and remain 10 features for SEI using stable signals. We call it the comparative Method 2. We compare the proposed method with these two methods at the same condition to verify the performance of proposed method. The experimental signals include measured signals and simulated signals. The measured signals are 6 kinds of ship signals collected from a department, which are labeled with ①~⑥ for identification experiment.

Liu et al. [15] point out that nonlinear characteristics are unique in each emitter which can be described using Taylor polynomials. In [13], an emitter signal simulation model is proposed based on Taylor polynomial. It attributes the unique features of emitters to the nonlinear response in power amplifier. Let D_s be the order of the Taylor polynomial .A simulated emitter signal can be described as:

$$\mathrm{G}(d(n)) = \sum_{l=1}^{D_s} \alpha_l (d(n))^l, \tag{23}$$

$G(d(n))$ is the output signal at the power amplifier and $\{\alpha_l\}$ are the coefficients of the Taylor polynomial . $d(n)$ is the input signal at the power amplifier .It's a kind of modulated signal described as

$$d(n) = x_n e^{j2\pi n \frac{f_c}{f_s}}. \tag{24}$$

$x(n)$ is the baseband signal at time n and here we choose QPSK modulation format as the baseband signal in our simulation. f_c is the carrier frequency and f_s is the sampling frequency of narrow-band signal. It's clear that for the same order D_s, different coefficients represent the different RF fingerprints of emitters. In our simulation model, the order of Taylor polynomial D_s is set at 3.We use coefficient $\boldsymbol{\alpha}^{[1]}$=[1, 0.5, 0.3], $\boldsymbol{\alpha}^{[2]}$=[1, 0.08, 0.6], $\boldsymbol{\alpha}^{[3]}$=[1, 0.01, 0.01] $\boldsymbol{\alpha}^{[4]}$=[1, 0.01, 0.8] and $\boldsymbol{\alpha}^{[5]}$=[1, 0.6, 0.04] to simulate 5 kind of different emitter signals. We set the sampling frequency f_s at 100MHz and carrier frequency f_c at 30MHz. Each simulated signal contains 10000 QPSK symbols. We test the algorithm performance in additive white Gaussian noise (AWGN) channel and single path Rayleigh fading channel with the Signal to Noise Ratio (SNR) changed. The maximum Doppler shift in Rayleigh channel is set at 50Hz. We use parameter *K* to represent the type of simulated signals for identification. For *K*=3, the simulated signals with coefficients $\boldsymbol{\alpha}^{[1]}$, $\boldsymbol{\alpha}^{[2]}$ and $\boldsymbol{\alpha}^{[3]}$ are used for identification experiment, for *K*=4, it is $\boldsymbol{\alpha}^{[1]}$,$\boldsymbol{\alpha}^{[2]}$, $\boldsymbol{\alpha}^{[3]}$, $\boldsymbol{\alpha}^{[4]}$ and for *K*=5,it is $\boldsymbol{\alpha}^{[1]}$,$\boldsymbol{\alpha}^{[2]}$, $\boldsymbol{\alpha}^{[3]}$, $\boldsymbol{\alpha}^{[4]}$, $\boldsymbol{\alpha}^{[5]}$.

B. Experimental Design

Regardless of simulated signals or measured signals, the number of training samples and test samples are both set to 100 for each class, and the length of each sample is set to 512 points. The number of time bins in TFED spectrum is the same as the length of each signal sample, and the number of frequency bins of the TFED spectrum is set to 400. So the size of each TFED spectrum sample is 512×400. For the measured signals, we randomly select training samples and test samples without repetition in each recognition experiment. Each recognition rate is the mean value of 80 times repeated experiments. For the simulated signals, we find that the recognition rate is related to the randomly generated symbol sequence under the same SNR. Thus, we firstly generate 40 groups of simulated emitter signals, and then repeat the recognition experiments for 20 times using each group of simulated signals. Each acquisition of recognition rate is the average value of 800 times experiments.

Authorized licensed use limited to: ULAKBIM UASL - Bogazici Universitesi. Downloaded on December 07,2020 at 21:24:35 UTC from IEEE Xplore. Restrictions apply.

C. Experimental Results

The relationship between the number of training samples for each class and the identification accuracy are plotted in Fig. 2. Here, we set the test samples for each class at 100 fixedly and change the number of training samples for each class at 50,100,150,200. Four kinds of simulated signals and measured ship signals are used to test the performance of proposed method against to the number of training samples. For simulated signals, we conduct the experiment at 15dB in AWGN channel and Rayleigh channel respectively, which reduces the influence of too high or too low SNR on results. For measured ship signals, two sets of signals with label ②④⑤⑥ and ①②④⑤ are used for experiment. The recognition rate hardly changes on simulated signals and measured ship signals. This result indicates that the number of training samples barely influences the recognition rate. The extracted RF fingerprints is robust against the training samples.

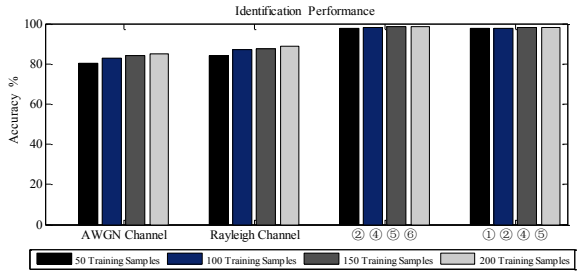

Figure 2. The relationship between recognition rate and the number of training samples:4 types of simulated signals in AWGN channel and Rayleigh channel SNR=15dB; 4 types of measured ship signals with the number of training samples N=50,100,150,200.

Fig. 3-Fig. 5 show the identification performance of 3 SEI methods in AWGN channel and Rayleigh channel. For $K=3$ in AWGN channel, only the proposed method can get more than 80% accuracy for SNR=10dB. The proposed method gets 99.55% accuracy for SNR=20dB, while Method 1 and Method 2 only get 85.53% and 88.74%,respectively. The identification performance of 3 SEI methods declines in Rayleigh channel as a whole, but the proposed method and method 2 get a higher performance than in AWGN channel at low SNR, such as SNR=5dB and SNR=10dB. For $K=4$ in AWGN channel, the proposed method gets more than 90% accuracy for SNR=20dB. However, Method 1 and Method 2 get less than 80% only. For K=4 in Rayleigh channel, the proposed method can get about 95% accuracy for SNR=30dB, but Method 1 and Method 2 only get about 80% and 89%, respectively. We can find that all the three methods nearly reach the bottleneck of accuracy but the proposed method has better performance obviously. We can make some similar analysis for K=5. From a series of experiments, we can find that whether in AWGN channel or in Rayleigh channel, the identification accuracy of the proposed method is higher than the accuracy of another two methods, especially at low SNR. With the increase of signal types for identification, the recognition rate decreases in all three methods, but the proposed method gets the best performance in AWGN channel or Rayleigh channel. Besides, the identification accuracy gap becomes wider between the proposed method and another two methods.

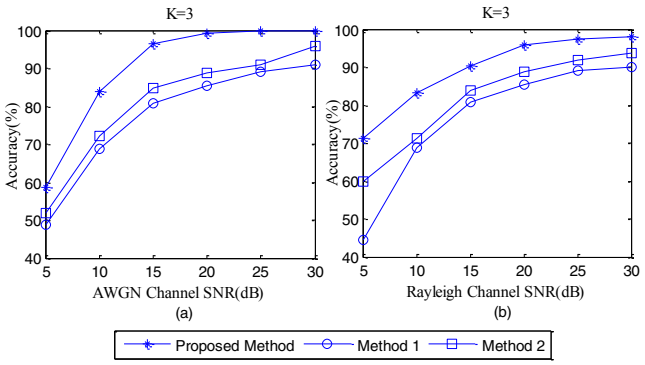

Figure 3. The identification performance comparison among 3 SEI methods: (a) shows the identification performance in AWGN channel; (b) shows the identification performance in Rayleigh channel.

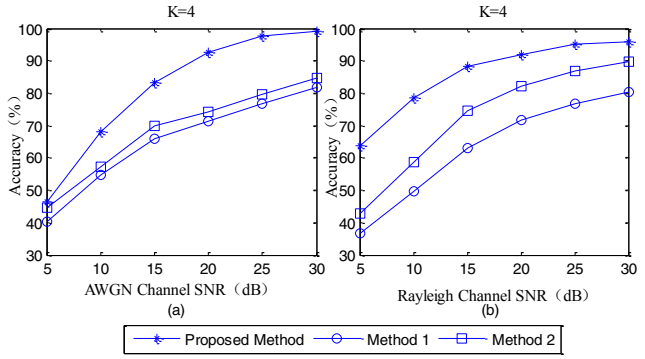

Figure 4. The identification performance comparison among 3 SEI methods: (a) shows the identification performance in AWGN channel; (b) shows the identification performance in Rayleigh channel.

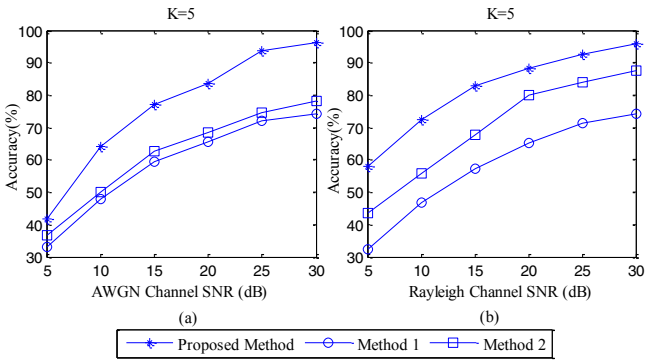

Figure 5. The identification performance comparison among 3 SEI methods: (a) shows the identification performance in AWGN channel; (b) shows the identification performance in Rayleigh channel.

We randomly select several signals from 6 kinds of measured ship signals for experiment. The experiment results are partly shown in Table I. It's further demonstrated that the proposed method gets a better performance.

Authorized licensed use limited to: ULAKBIM UASL - Bogazici Universitesi. Downloaded on December 07,2020 at 21:24:35 UTC from IEEE Xplore. Restrictions apply.

TABLE I. IDENTIFICATION PERFORMANCE ON MEASURED SHIP SIGNALS

Measured ship signals for experiment						Proposed Method	Comparative Method 1	Comparative Method 2
③	⑤	⑥				95.23%	88.11%	91.01%
①	②	④				99.61%	94.67%	96.43%
①	⑤	⑥				96.55%	84.20%	96.45%
②	③	④	⑥			90.18%	87.32%	88.65%
①	②	④	⑥			96.55%	91.92%	96.05%
①	④	⑤	⑥			97.17%	87.68%	93.90%
①	②	③	④	⑤		93.57%	88.15%	91.15%
②	③	④	⑤	⑥		91.82%	85.48%	87.46%
①	②	④	⑤	⑥		97.03%	84.30%	92.75%
①	②	③	④	⑤	⑥	90.94%	82.26%	87.76%

V. CONCLUSION AND OUTLOOK

In this paper, we propose a method extracting RF fingerprints for SEI，which extracts texture features by converting the TFED spectrum into a image. When compared with another two methods based on EMD, the proposed method provides better identification performance. However, there are still some aspects need to be improved in our algorithm. We only utilize several simple texture features and there are lots of redundancy and correlation in them. We decide to extract some other texture features and reduce the dimensions of extracted features by PCA and so on. Moreover, we will test the identification performance in more complex condition like non-Gaussian channel or Multipath Rayleigh fading channel and use other modulation format for experiment next.

ACKNOWLEDGMENT

The authors would like to thank the reviewers for their insightful comments and helpful suggestions.

REFERENCES

[1] Langley LE.“Specific emitter identification (SEI) and classical parameter fusion technology” Wescon/93 Conference Record. Apr,1993pp.377-381

[2] Ellis K J,Serinken N. “Characteristics of radio transmitter fingerprints” . Radio Science, vol. 36, Jun .2001,pp.585-598.

[3] Danev B, Luecken H, Capkun S. “Attacks on physical-layer identification” ACM Conference on Wireless Network Security, WISEC 2010, Hoboken, New Jersey, USA, March. 2010,pp.89-98.

[4] Kim K, Spooner C M, Akbar I, JH Reed. “Specific Emitter Identification for Cognitive Radio with Application to IEEE 802.11”Global Communication Conference 2008.,vol.49 ,Aug.2008, pp.1-5.

[5] Liu M W, Doherty J F. “Specific Emitter Identification using Nonlinear Device Estimation” Sarnoff Symposium. IEEE,Feb, 2008,pp.1-5.

[6] Li L, Ji H B, Jiang L. “Quadratic time-frequency analysis and sequential recognition for specific emitter identification” IET Signal Processing,vol.6 ,May.2011, pp.568-574.

[7] Huang, N.E, Shen Z ,et al.. “The empirical mode decomposition and the Hilbert spectrum for nonlinear and non-stationary–time series analysis”.Proc.R.Soc.Lond.A,vol.454,Sep.1998,pp. 903-995.

[8] Zheng T X, Yang L H. “Discussion and Improvement on Empirical Mode Decomposition Algorithm “. Acta Scientiarum Natralium Universitatis Sunyatseni, vol.46,Jul.2007,pp.1-6.

[9] Mark G. Frei. “Intrinsic time-scale decomposition: time-frequency-energy analysis and real-time filtering of non-stationary signals”Proceedings of the Royal Society A Mathematical Physical & Engineering Sciences, vol.463,Apr.2007, pp.321-342.

[10] Song C, Zhan Y, Guo L. “Specific emitter identification based on Intrinsic Time-Scale Decomposition” International Conference on Wireless Communications Networking and Mobile Computing. IEEE, Nov.2010,pp.1-4.

[11] Ge J. “Research on image texture feature extraction and classification algorithm” Tianjin University, Jun.2010

[12] Cortes C, Vapnik V. “Support-Vector Networks” Machine Learning. Nov.1995,pp.273-297.

[13] Zhang J, Wang F, Dobre O A,Zhangdui zhong. “Specific emitter identification via Hilbert–Huang Transform in Single-Hop and Relaying Scenarios” IEEE Transactions on Information Forensics & Security,vol.6, Nov.2016, pp.1192-1205.

[14] Yuan Y, Huang Z, Wu H.”Specific emitter identification based on Hilbert-Huang transform-based time-frequency-energy distribution features “.IET Communications, vol.13,Aug.2014, pp.2404-2412.

[15] Liu M W, Doherty J F. “Nonlinearity estimation for specific emitter identification in multipath environment” IEEE Sarnoff Symposium. IEEE Press, Jan.2009,pp.1076-1085.

Authorized licensed use limited to: ULAKBIM UASL - Bogazici Universitesi. Downloaded on December 07,2020 at 21:24:35 UTC from IEEE Xplore. Restrictions apply.